

Dark-matter halo mergers as a fertile environment for low-mass Population III star formation

S. Bovino^{*1}, M. A. Latif¹, T. Grassi², and D. R. G. Schleicher¹

¹*Institut für Astrophysik Georg-August-Universität, Friedrich-Hund Platz 1, D-37077 Göttingen, Germany*

²*Centre for Star and Planet Formation, Natural History Museum of Denmark, Øster Voldgade 5-7, DK-1350 Copenhagen, Denmark*

³*Department of Chemistry, Sapienza University of Rome, P.le A. Moro, I-00185, Rome, Italy*

Accepted *****. Received *****; in original form *****

ABSTRACT

While Population III stars are typically thought to be massive, pathways towards lower-mass Pop III stars may exist when the cooling of the gas is particularly enhanced. A possible route is enhanced HD cooling during the merging of dark-matter halos. The mergers can lead to a high ionization degree catalysing the formation of HD molecules and may cool the gas down to the cosmic microwave background (CMB) temperature. In this paper, we investigate the merging of mini-halos with masses of a few $10^5 M_\odot$ and explore the feasibility of this scenario. We have performed three-dimensional cosmological hydrodynamics calculations with the ENZO code, solving the thermal and chemical evolution of the gas by employing the astrochemistry package KROME. Our results show that the HD abundance is increased by two orders of magnitude compared to the no-merging case and the halo cools down to ~ 60 K triggering fragmentation. Based on Jeans estimates the expected stellar masses are about $10 M_\odot$. Our findings show that the merging scenario is a potential pathway for the formation of low-mass stars.

Key words: cosmology: theory – Pop III, astrochemistry – ISM: , molecules – methods: numerical – evolution.

1 INTRODUCTION

The formation modes of the first generations of stars have been a challenging subject for many years and today still represent a central topic of research in modern cosmology. The current understanding is that these stars were formed in mini-halos of about $10^6 M_\odot$ around $z = 20$ – 30 , which is strongly supported by many numerical simulations performed over the years (Abel et al. 2002; Bromm et al. 2002; Ciardi & Ferrara 2005; Yoshida et al. 2006; O’Shea & Norman 2007; Greif et al. 2008, 2012). Since Saslaw & Zipoy (1967), it is widely accepted that the collapse process leading to the formation of these early objects is mainly driven by H_2 cooling (Peebles & Dicke 1968; Palla et al. 1983). Due to the lack of a permanent dipole moment the hydrogen molecule becomes an ineffective coolant below ~ 200 K when it reaches the local thermodynamic equilibrium (LTE). Considering these thermal conditions, it has been postulated that the final mass of the first generation of stars should be of the order of $\sim 100 M_\odot$ or more, with a resultant short life (Abel et al. 2002; Bromm et al. 2002; Bromm 2013). Recent numerical simulations (Clark et al.

2011; Greif et al. 2012; Stacy et al. 2012) suggest that the characteristic mass scale of the first stars should be lowered to several ten solar masses. The large parameter study by Hirano et al. (2014) indicates a significant spread around this mass scale, and extreme values up to $1000 M_\odot$.

Comprehending the conditions under which the first stars were formed is very important to study the early history of the Universe as they initiated cosmic reionization and the enrichment of the intergalactic medium (e.g. Barkana & Loeb 2001; Schneider et al. 2006; Schleicher et al. 2008), and may also have seeded the formation of supermassive black holes (Li et al. 2007; Volonteri 2012; Latif et al. 2013a; Hosokawa et al. 2013; Latif et al. 2013e).

Many authors (Bromm et al. 2002; Johnson & Bromm 2006; Yoshida et al. 2006; Ripamonti 2007; Greif et al. 2008; McGreer & Bryan 2008) also discussed the possible role of HD as an additional coolant which may have led to the formation of lower-mass stars. They found that in the presence of a higher electron abundance, HD cooling can become efficient allowing the gas to reach the temperature of the CMB. The need of a high ionization fraction suggested the introduction of a second mode to form primordial stars named Pop III.2 to be distinguished from Pop III.1 in which

* Corresponding author: sbovino@astro.physik.uni-goettingen.de

H_2 cooling dominates throughout (see Tan & McKee 2008; Bromm 2013). The Pop III.2 stars are then expected to be assembled from a gas which is still metal-free but embedded in ionized environments. The latter may be triggered by the explosions of the first supernovae or HII regions or strong shocks (e.g. Mackey et al. 2003; Yoshida et al. 2007; Greif et al. 2008). Lower-mass stars may also be formed within the Pop III.1 paradigm as shown by Hirano et al. (2014). They suggested that in a slowly collapsing cloud the compressional heating is reduced and may create the conditions for the HD cooling to become effective. In some of the above mentioned papers (Bromm et al. 2002; Ripamonti 2007; McGreer & Bryan 2008) the authors claimed that in mini-halos of a few $\sim 10^5 M_\odot$ under certain circumstances (temperature below ~ 200 K at densities of at least 10^4 cm^{-3}), HD can efficiently be formed and overcome the H_2 cooling rate. Stacy & Bromm (2013) performed cosmological simulations of the formation and growth of Pop III stellar systems and argued that a mini-halo formed at redshift 15 and supported by high baryonic angular momentum can lead to the formation of 1-5 M_\odot stars. Lower-mass stars are thus also included in the expected scatter of the Pop III.1 distribution.

McGreer & Bryan (2008) concluded that in halos with masses $> 10^6 M_\odot$ the cooling is dominated by H_2 and the final stars could have a mass of $\sim 100 M_\odot$, while for lower mass halos of $\sim 10^5 M_\odot$ HD cooling becomes important and leads to stellar masses between 10-40 M_\odot . However, the occurrence of such low-mass systems was found to be less frequent. These conclusions are in overall agreement with the simplified numerical simulation (1D Lagrangian) reported by Ripamonti (2007) and with the robust statistical study presented by Hirano et al. (2014).

The main idea behind the possible role of HD in primordial star formation comes from the series of chemical reactions which leads to the formation of HD. This is strongly related to the ionization fraction because the main formation path for HD is



as largely discussed in earlier papers (Stancil et al. 1998; Galli & Palla 2002; Gay et al. 2011). The only way to trigger the formation of HD is then to boost the formation of H_2 pumping the main reactive channel which is directly linked to H^- via the following reactions:



In addition the formation and destruction of D^+ should be considered



This leads to the conclusion that a high ionization fraction boosts the formation of HD via a chain of chemical events that includes the key species in the following way $\text{e}^- \rightarrow \text{H}^- \rightarrow \text{H}_2 \rightarrow \text{HD}$.

Another possible route for primordial star formation (Pop III.2) which also involves the HD cooling has been proposed by Shchekinov & Vasiliev (2006), and Prieto et al. (2012, 2014). The idea suggested by Shchekinov & Vasiliev (2006) is based on the merging of dark-matter halos within

the context of the hierarchical scenario of structure formation (Barkana & Loeb 2001; Ciardi & Ferrara 2005). Merging induces compression and the consequent formation of shock-waves which may enrich the baryonic component of the gas by free electrons catalyzing the HD formation. The authors consider a simplified one-dimensional model where two identical halos collide and follow the non-equilibrium evolution of the HD behind the shock-waves which formed during the merging process. In these halos, they further assume a uniform density equal to the virial density. They found that to have a higher ionization degree and to boost the formation of HD the merger masses should be $M > 8 \times 10^6 [(1+z)/20]^{-2} M_\odot$. In a real merger, we however expect a more complex density structure, and the strength of the shocks is likely enhanced in the central regions. Their mass scale can therefore just serve as a rough estimate. In a recent study, Prieto et al. (2012, 2014) performed cosmological N-body simulations and computed the statistic of the halos fulfilling the Shchekinov & Vasiliev (2006) criterion. Their findings suggest that the fraction of halos going through this phase is significant.

In this paper we investigate the role of HD as a coolant in post-shocked environments generated by dark-matter halo merging. In particular we consider a merger of more than two halos with masses well below the threshold set by Shchekinov & Vasiliev (2006) and run self-consistent cosmological simulations, following both the merging and the collapsing process with enough accuracy to capture important chemo-dynamical features.

The paper is organized as follow: we first introduce the methodology and the chemical model involved in the cosmological simulations, then discuss the main results, and finally give our conclusions.

2 METHODOLOGY

To follow the merger and collapse of a halo from cosmological initial conditions we use the hydrodynamic code **ENZO**, version 2.3 (The Enzo Collaboration et al. 2013). **ENZO** is based on an adaptive mesh refinement (AMR) method and it is well-tested in the framework of cosmological simulations of primordial star formation (Abel et al. 2002; O’Shea & Norman 2007; Turk et al. 2009; Latif et al. 2013c). It includes the split 3rd-order piece-wise parabolic (PPM) method for solving the hydrodynamical equations, while the dark matter component is modeled using the particle-mesh technique. Self-gravity is calculated via a multigrid Poisson solver.

Our approach is divided in different steps. We first run a dark-matter only low-resolution simulation to study the evolution and the merging history of the halos. A single box of 1.0 comoving Mpc with a top grid resolution of 128^3 cells is employed. The parameters for creating the initial conditions and the distribution of baryonic and dark matter components are taken from the WMAP seven year data (Jarosik et al. 2011). We select a final mini-halo of mass $\sim 7 \times 10^5 M_\odot$ as a possible site of first star formation by using the halo finder implemented in the YT package (Turk et al. 2011) and based on the HOP algorithm by Eisenstein & Hu (1999). Then we re-run our simulation with the box centered in the selected mini-halo adding two additional nested

Table 1. Chemical network employed in the simulations.

Reactions	
1) $\text{H} + \text{e}^- \rightarrow \text{H}^+ + 2\text{e}^-$	15) $\text{H}^- + \text{H} \rightarrow 2\text{H} + \text{e}^-$
2) $\text{H}^+ + \text{e}^- \rightarrow \text{H} + \gamma$	16) $\text{H}^- + \text{H}^+ \rightarrow 2\text{H}$
3) $\text{He} + \text{e}^- \rightarrow \text{He}^+ + 2\text{e}^-$	17) $\text{H}^- + \text{H}^+ \rightarrow \text{H}_2^+ + \text{e}^-$
4) $\text{He}^+ + \text{e}^- \rightarrow \text{He} + \gamma$	18) $\text{H}_2^+ + \text{e}^- \rightarrow 2\text{H}$
5) $\text{He}^+ + \text{e}^- \rightarrow \text{He}^{2+} + 2\text{e}^-$	19) $\text{H}_2^+ + \text{H}^- \rightarrow \text{H} + \text{H}_2$
6) $\text{He}^{2+} + \text{e}^- \rightarrow \text{He}^+ + \gamma$	20) $3\text{H} \rightarrow \text{H}_2 + \text{H}$
7) $\text{H} + \text{e}^- \rightarrow \text{H}^- + \gamma$	21) $\text{H}_2 + 2\text{H} \rightarrow 2\text{H}_2$
8) $\text{H}^- + \text{H} \rightarrow \text{H}_2 + \text{e}^-$	22) $\text{H}^+ + \text{D} \rightarrow \text{H} + \text{D}^+$
9) $\text{H} + \text{H}^+ \rightarrow \text{H}_2^+ + \gamma$	23) $\text{H} + \text{D}^+ \rightarrow \text{H}^+ + \text{D}$
10) $\text{H}_2^+ + \text{H} \rightarrow \text{H}_2 + \text{H}^+$	24) $\text{H}_2 + \text{D}^+ \rightarrow \text{HD} + \text{H}^+$
11) $\text{H}_2 + \text{H}^+ \rightarrow \text{H}_2^+ + \text{H}$	25) $\text{HD} + \text{H}^+ \rightarrow \text{H}_2 + \text{D}^+$
12) $\text{H}_2 + \text{e}^- \rightarrow 2\text{H} + \text{e}^-$	26) $\text{H}_2 + \text{D} \rightarrow \text{HD} + \text{H}$
13) $\text{H}_2 + \text{H} \rightarrow 3\text{H}$	27) $\text{HD} + \text{H} \rightarrow \text{H}_2 + \text{D}$
14) $\text{H}^- + \text{e}^- \rightarrow \text{H} + 2\text{e}^-$	28) $\text{D} + \text{H}^- \rightarrow \text{HD} + \text{e}^-$

grids. As we want to follow the merging process leading to our mini-halo we adopt a refinement strategy which copes with the computational demands of these calculations. From $z = 99$ to $z = 12$ (the time at which the merging processes is almost over) we allow 21 levels of refinement and 32 cells per Jeans length. With the same resolution we then follow the evolution of the mini-halo until a density of 10^8 cm^{-3} , the range of interest to study the effect of HD cooling. Our refinement strategy is based on overdensity, Jeans length, and particle mass and is applied during the course of the simulations to ensure that all physical processes like shock waves and Truelove criterion (Truelove et al. 1997) are well resolved. A final resolution of $\sim 190 \text{ AU}$ in comoving is achieved.

2.1 Chemical model

The chemical and thermal evolution of the gas is consistently solved along with the hydrodynamical equations by employing the astrochemistry package **KROME** (Grassi et al. 2013). The latter is well suited for the study of many chemical environments and employs very accurate and efficient solvers as already shown and discussed in previous works (Bovino et al. 2013; Grassi et al. 2013; Bovino et al. 2014). To include **KROME** in **ENZO** we used the patch directly provided by **KROME** and publicly released with the package¹. Our chemical network includes 28 reactions, listed in table 1, and 12 species: H , H^+ , H^- , H_2 , H_2^+ , He , He^+ , He^{2+} , e^- , D , D^+ , and HD . The reaction rates are the same already discussed in many papers employing the **ENZO** code (for details see Anninos et al. 1997; Ripamonti 2007). The only difference lies on the H_2 three-body formation rate: we employ the latest accurate available rate from Forrey (2013a,b) which has already been tested in primordial star formation studies in a recent paper (Bovino et al. 2014). Heating and cooling include: H_2 formation heating as described in Omukai et al. (2005), H_2 cooling as reported in Glover & Abel (2008), bremsstrahlung, H and He line cooling (Cen 1992), HD cooling by Lipovka et al. (2005), and collisionally induced

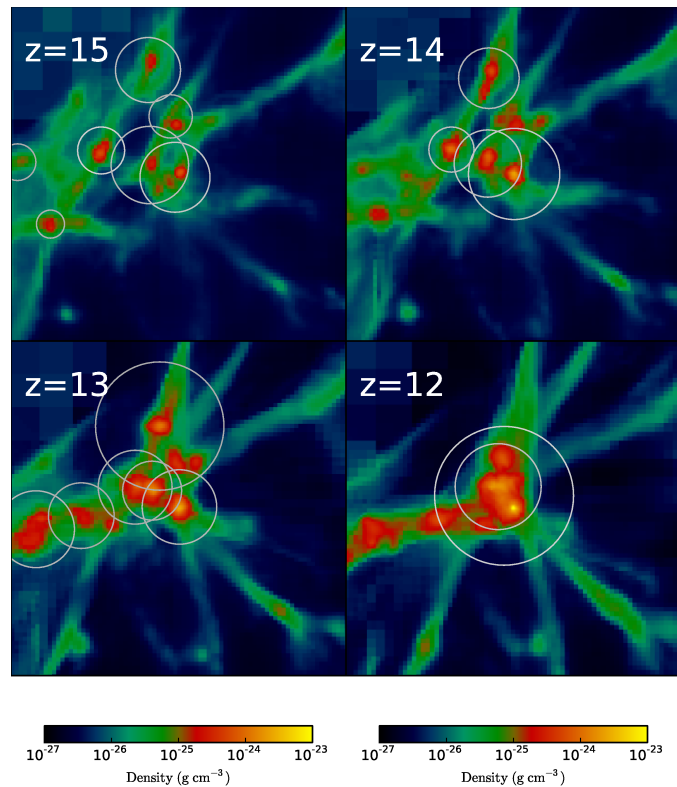


Figure 1. Density projections showing the merging of various halos at different redshifts. The overplotted circles represent halos of at least a few $10^5 M_\odot$ and the plot scale is 2 kpc.

emission (CIE) cooling as discussed in Grassi et al. (2013). In addition, we include the optically thick correction for the H_2 cooling following Ripamonti & Abel (2004) and Grassi et al. (2013). More details about the cooling and the heating functions can be found in the **KROME** paper (Grassi et al. 2013) where they are extensively discussed. It is worth noting that the atomic cooling and the CIE process, as well as the optical thick correction, are not important in this study as we look at an intermediate range of densities, $10^4 < n < 10^8 \text{ cm}^{-3}$, while the above contributions play an important role in the high-density regime ($n > 10^8 \text{ cm}^{-3}$). We decided to include them anyway for the sake of completeness.

To accurately solve the evolution of the chemical species and the temperature, we employ the following tolerances for the **DLSODES** solver: a relative tolerance $\text{RTOL}=10^{-4}$, and an absolute tolerance $\text{ATOL}=10^{-10}$. These tolerances ensure good performance without losing accuracy.

3 RESULTS

In Fig. 1, we show the merging of halos with more than $10^5 M_\odot$ at different redshifts ranging from $z = 15 - 12$. The merging process is initiated around redshift $z = 15$ where several halos of a few 10^5 solar masses start to interact. The process gradually continues along the gas filaments and 4-5 halos converge towards the central region until $z = 12$, where we clearly see two mini-halos, as depicted by the circles. The

¹ Webpage **KROME**: <http://kromepackage.org>

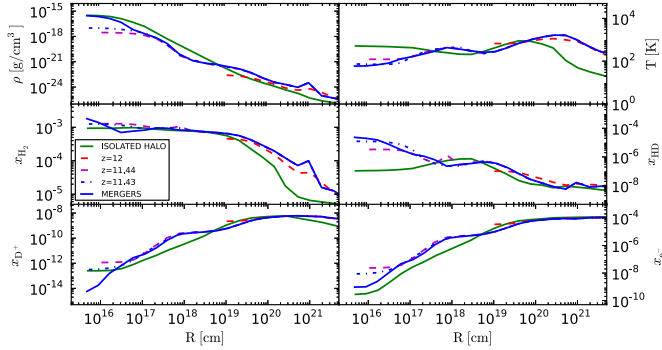


Figure 2. Radially averaged profiles for density (top left), temperature (top right), H_2 (middle left), HD (middle right), D^+ (bottom left), and electron (bottom right) mass fractions, for different redshifts. The comparison between the isolated run (green solid) and the mergers (blue solid) is made taking the data at the same density peak in the simulations. See text for details.

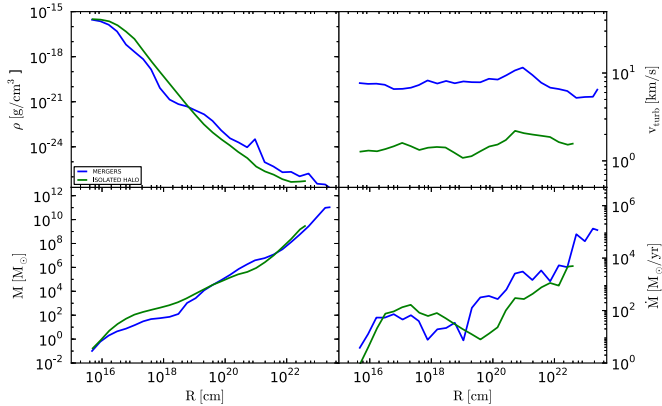


Figure 3. Radially averaged profiles for density (top left), turbulent velocity in km s^{-1} (top right), total mass in solar masses (bottom left), and accretion rate in $\text{M}_\odot \text{ yr}^{-1}$ (bottom right) for the isolated halo (blue dashed) and the mergers run (red solid) for the last dump in the simulation. The comparison data are taken at the same peak density.

latter merge together to form a mini-halo of $7 \times 10^5 \text{ M}_\odot$. Note here that the size of the circles corresponds to the physical mass of the halos and is provided by the halo finder employed in YT; bigger circles represent more massive halos. We then follow the evolution of the halo from the last merging process until density of 10^8 cm^{-3} with the aim to capture the effect of the post-shocked environment created by the mergers. The results obtained are reported in Fig. 2 at different times. As we are interested in examining in detail the effect of the merging process on the chemical and thermal evolution

of the simulated halo, we plot the radially averaged mass fractions of the most important species (H_2 , HD, D^+ , e^-), as well as the temperature and the density profiles. To better understand the chemical behaviour, we also performed a run for an isolated mini-halo with mass roughly equal to the merger case, employing the same chemical network, as well as the same thermal processes. The initial conditions for the above isolated halo are taken from our previous work (see halo C in Bovino et al. 2013, 2014; Grassi et al. 2013) and the results from this run are also shown in Fig. 2. The comparison is made by taking the data at the same peak density.

It is clearly seen from Fig. 2 that a high ionization degree is produced by the shocks created during the merging process. Compared to the isolated halo run the electron fraction is, indeed, almost one order of magnitude higher for a radius between 10^{-2} and 1 pc, catalysing the formation of H_2 and HD. As discussed in §1 the only way to boost the formation of HD is the presence of a high electron fraction which initiates the following chemical chain reaction $\text{H}^- \rightarrow \text{H}_2 \rightarrow \text{HD}$. The fraction of HD is $\sim 10^{-5}$ in the mergers case compared to $\sim 10^{-7}$ for the isolated case, while the H_2 fraction is about a factor of two higher for the merger. The overall $[\text{H}_2/\text{HD}]$ ratio is 10^4 in the case of the isolated halo and 10^2 in the case where mergers are considered, which results in about two orders of magnitude increase in the HD abundance. The thermal evolution is then a consequence of the chemical evolution. Having HD a hundred times more abundant allows this molecule to cool the gas below 200 K, the temperature where H_2 reaches the LTE. The temperature in the core is about 60 K for the mergers case, while for the isolated halo the temperature remains higher (i.e. ~ 500 K at the same densities). For the merger run, a higher temperature is noted at about 1 kpc scale due to the heating by post-merging shocks. As a result of the lower temperature in the core the electron abundance declines by one order of magnitude in 0.25 Myr (from $z = 11.44$ to $z = 11.43$) due to recombination processes.

The dynamical properties of the halo are reported in Fig. 3 for both the merger and the isolated halo. Density profiles for both runs are roughly similar and follow an R^{-2} behaviour corresponding to an isothermal collapse, with small deviations for the merger due to the additional fragmentation in the halo. As expected, the total mass (reported in the bottom left panel) increases as $\sim R$ in both cases, and deviations are related to the density profile where shocks are visible for the merger. The accretion rate is very large on the outer region and decreases to $10^{-1} \text{ M}_\odot/\text{yr}$ in the core as already reported in previous studies (Latif et al. 2013a,b). In the top right panel we report the turbulent velocity in km/s which is much higher for the merger run. The high turbulent velocity might be due to the presence of the two fragments which induces strong accretion flows. In the case of mergers the halo goes, in fact, through a fragmentation phase as shown in the bottom left panel of Fig. 4 where projections of the density, temperature, and HD mass fraction, at a scale of 10 pc are shown.

Multiple small clumps are formed in the center of the halo out of which two are visible in Fig. 4. As we are averaging the density along the direction of the projection the third clump is not clearly visible. The clump masses are of about 22, 23 and 0.15 M_\odot and the most massive one is gravitation-

ally bound and has higher rotational support. The central clump shows a very high HD fraction (about 10^{-4}) and a temperature of 60 K in the center due to the efficient HD cooling.

The calculations become computationally too expensive at later stages for densities higher than 10^8 cm^{-3} and a sink particle approach should be employed to follow the evolution for longer times (e.g. Smith et al. 2011). At that point, incorporating feedback from the accretion luminosity would also be relevant. Nevertheless the effect of the HD cooling on the thermal history of the halo is accurately represented if we consider that HD reaches the LTE around 10^8 cm^{-3} , so that the simulation is well-suited to study the initial fragmentation.

4 CONCLUSIONS AND DISCUSSION

In this paper we follow the evolution of a mini-halo of $\sim 7 \times 10^5 M_\odot$ formed from the merging of a number of halos with masses of a few $10^5 M_\odot$. It was in fact suggested (Shchekinov & Vasiliev 2006) that if two massive enough halos collide and merge the gas can go through a post-shocked ionized stage which boosts the formation of the HD molecule then allowing the gas to cool below 200 K. As the final mass of the first luminous objects is given by the Jeans mass

$$M_J = 500 M_\odot \left(\frac{T}{200 \text{ K}} \right)^{3/2} \left(\frac{10^4 \text{ cm}^{-3}}{n} \right)^{1/2} \quad (5)$$

it is clear that in an environment dominated by H_2 cooling the expected mass is of about $500 M_\odot$ (assuming $T = 200 \text{ K}$ and $n = 10^4 \text{ cm}^{-3}$), while for the HD cooling case the mass is lowered to $\sim 10 M_\odot$ (e.g. assuming a temperature of 60 K at $n \sim 10^6 \text{ cm}^{-3}$).

A first attempt to investigate the statistics of the halo going through a merging process has been made by Prieto et al. (2014) within a cosmological framework.

Here we go beyond this study by coupling the solution of dark matter and hydrodynamics (solved with **ENZO**) with an accurate treatment of the non-equilibrium chemistry (solved by **KROME**). We performed high-resolution cosmological simulations for a box of 1 comoving Mpc and follow the evolution of the halo starting from $z = 99$, going through the end of the merging process around $z = 12$. We finally follow the collapse until a gas density of 10^8 cm^{-3} where HD cooling is known to usually dominate (Lipovka et al. 2005; Glover & Abel 2008).

Our results clearly show that the shock-waves generated by the merging process increase the ionization fraction catalyzing the formation of HD via H_2 . We found a HD abundance two orders of magnitudes larger than the one obtained with an isolated halo setup. As a consequence, the temperature in the core dropped down to 60-70 K, much lower compared to the isolated halo run where the gas is hotter (around $\sim 500 \text{ K}$). Such over-cooling in the halo has induced fragmentation and multiple clumps are observed, out of which two are rotationally supported and one is gravitationally bound.

It is quite interesting to note that a merging process involving several halos with masses of few $10^5 M_\odot$ can similarly produce high ionization degree as in the case proposed by Shchekinov & Vasiliev (2006) for more massive mergers.

These conditions are then sufficient to catalyze the required HD fraction. The differences in the masses of the mergers rise from the fact that we performed realistic three-dimensional calculations compared to the simplified one-dimensional estimates by Shchekinov & Vasiliev (2006) that provide only a qualitative picture of the process. In particular simplified one-dimensional models underestimate the strength of the merger shocks and do not take into account the collapse dynamics and the hydrodynamical effects (e.g. compressional heating). Another strong simplification is the assumption of a virial density while realistic halos are partially collapsed, enhancing the formation of molecules. Based on the halo finder results from the simulations we found a relative velocity of $\sim 7.0 \text{ km/s}$ between the dark matter halos which is about a factor of 1.5 larger than the estimate by Shchekinov & Vasiliev (2006) from their Eq. 2. Combining all these factors leads to a higher degree of ionization and enhanced formation of molecules even for low mass mergers. The present work therefore indicates a potential formation route for low-mass primordial stars due to merger-enhanced HD cooling. This pathway should be explored further in future studies, including a larger range of initial conditions.

While previous works (e.g. McGreer & Bryan 2008; Hirano et al. 2014) stated that the fraction of HD-cooled halos is negligible in primordial *unperturbed* environments, our findings suggest that the fraction of these halos might be larger than previously estimated as merger events are much more common in the early Universe.

Finally, the presence of high turbulent energy produced in the aftermath of merging event may also contribute to the amplification of magnetic fields through the so-called small scale dynamo process (Schober et al. 2012; Bovino et al. 2013; Schleicher et al. 2013; Latif et al. 2013; Schleicher et al. 2013; Latif et al. 2013d). The presence of such fields may further influence fragmentation and disk formation at higher densities (e.g. Machida & Doi 2013; Latif et al. 2013c).

ACKNOWLEDGEMENTS

S.B. and D.R.G.S. thank for funding through the DFG priority program ‘The Physics of the Interstellar Medium’ (project SCHL 1964/1-1). D.R.G.S. and M.L. thank for funding via the SFB 963/1 on ‘Astrophysical Flow Instabilities and Turbulence’ (project A12). The plot of this paper have been obtained by using the YT tool. The simulations have been performed on the Milky Way cluster at the Forschungszentrum Jülich. We all are grateful to J. Prieto for having inspired this work and for fruitful discussions.

REFERENCES

- Abel T., Bryan G. L., Norman M. L., 2002, *Science*, 295, 93
- Anninos P., Zhang Y., Abel T., Norman M. L., 1997, *New Astronomy*, 2, 209
- Barkana R., Loeb A., 2001, *Phys. Rep.*, 349, 125
- Bovino S., Grassi T., Latif M. A., Schleicher D. R. G., 2013, *MNRAS*, 434, L36

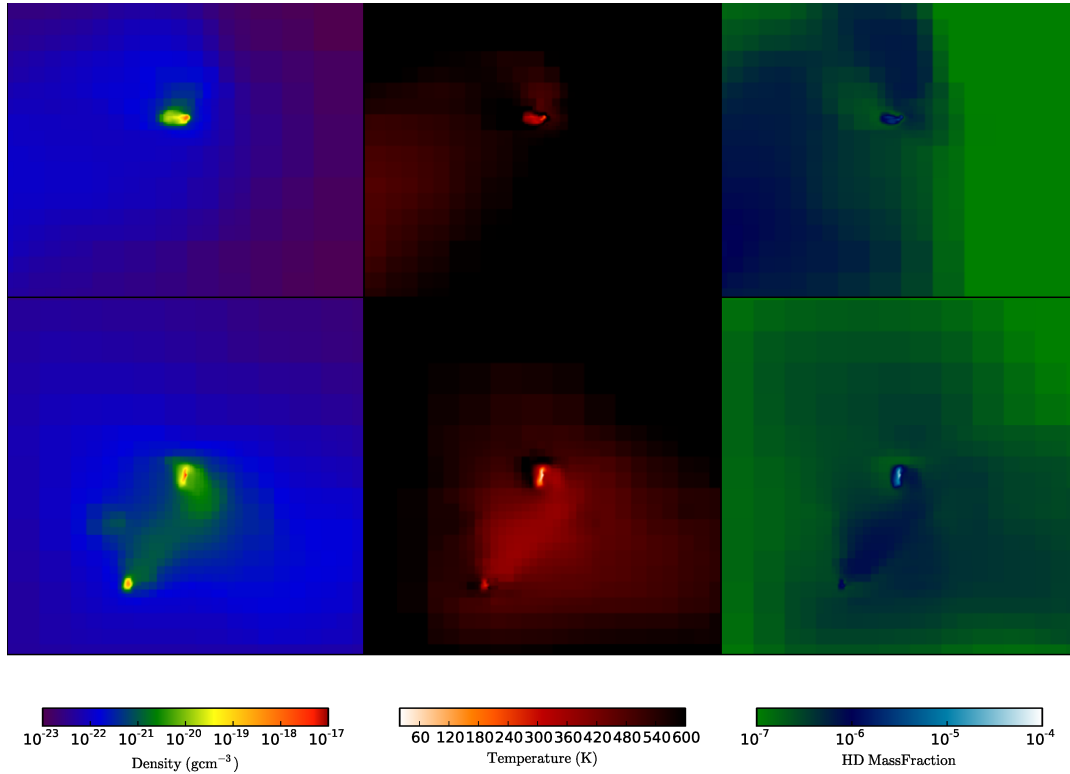


Figure 4. Density, temperature, and HD mass fraction projections, for the run where merging occurs at a scale of 10 pc for two different redshifts, $z = 1.44$ (upper panel), and $z = 11.43$ (lower panel).

Bovino S., Schleicher D. R. G., Grassi T., 2014, *A&A*, 561, A13
 Bovino S., Schleicher D. R. G., Schober J., 2013, *New Journal of Physics*, 15, 013055
 Bromm V., 2013, *Reports on Progress in Physics*, 76, 112901
 Bromm V., Coppi P. S., Larson R. B., 2002, *ApJ*, 564, 23
 Cen R., 1992, *ApJS*, 78, 341
 Ciardi B., Ferrara A., 2005, *Space Science Reviews*, 116, 625
 Clark P. C., Glover S. C. O., Smith R. J., Greif T. H., Klessen R. S., Bromm V., 2011, *Science*, 331, 1040
 Eisenstein D. J., Hu W., 1999, *ApJ*, 511, 5
 Forrey R. C., 2013a, *ApJL*, 773, L25
 Forrey R. C., 2013b, *Phys. Rev. A*, 88, 052709
 Galli D., Palla F., 2002, *P&SS*, 50, 1197
 Gay C. D., Stancil P. C., Lepp S., Dalgarno A., 2011, *ApJ*, 737, 44
 Glover S. C. O., Abel T., 2008, *MNRAS*, 388, 1627
 Grassi T., Bovino S., Schleicher D., Gianturco F. A., 2013, *MNRAS*, 431, 1659
 Grassi T., Bovino S., Schleicher D. R. G., Prieto J., Seifried D., Simoncini E., Gianturco F. A., 2013, *arxiv:1311.1070*
 Greif T. H., Bromm V., Clark P. C., Glover S. C. O., Smith R. J., Klessen R. S., Yoshida N., Springel V., 2012, *MNRAS*, 424, 399
 Greif T. H., Johnson J. L., Klessen R. S., Bromm V., 2008, *MNRAS*, 387, 1021
 Hirano S., Hosokawa T., Yoshida N., Umeda H., Omukai K., Chiaki G., Yorke H. W., 2014, *ApJ*, 781, 60

Hosokawa T., Yorke H. W., Inayoshi K., Omukai K., Yoshida N., 2013, *ApJ*, 778, 178
 Jarosik N., Bennett C. L., Dunkley J., Gold B., Greason M. R., Halpern M., Hill R. S., Hinshaw G., Kogut A., Komatsu E., Larson D., Limon M., Meyer S. S., Nolte M. R., Odegard N., Page L., Smith K. M., Spergel D., Tucker G. S., Weiland J. L., Wollack E., Wright E. L., 2011, *The Astrophysical Journal Supplement Series*, 192, 14
 Johnson J. L., Bromm V., 2006, *MNRAS*, 366, 247
 Latif M. A., Schleicher D. R. G., Schmidt W., 2013, *arxiv:1310.3680*
 Latif M. A., Schleicher D. R. G., Schmidt W., Niemeyer J., 2013a, *MNRAS*, 433, 1607
 Latif M. A., Schleicher D. R. G., Schmidt W., Niemeyer J., 2013b, *MNRAS*, 430, 588
 Latif M. A., Schleicher D. R. G., Schmidt W., Niemeyer J., 2013c, *ApJL*, 772, L3
 Latif M. A., Schleicher D. R. G., Schmidt W., Niemeyer J., 2013d, *MNRAS*, 432, 668
 Latif M. A., Schleicher D. R. G., Schmidt W., Niemeyer J., 2013e, *MNRAS*, 436, 2989
 Li Y., Hernquist L., Robertson B., Cox T. J., Hopkins P. F., Springel V., Gao L., Di Matteo T., Zentner A. R., Jenkins A., Yoshida N., 2007, *ApJ*, 665, 187
 Lipovka A., Núñez-López R., Avila-Reese V., 2005, *MNRAS*, 361, 850
 Machida M. N., Doi K., 2013, *MNRAS*, 435, 3283
 Mackey J., Bromm V., Hernquist L., 2003, *ApJ*, 586, 1
 McGreer I. D., Bryan G. L., 2008, *ApJ*, 685, 8

- Omukai K., Tsuribe T., Schneider R., Ferrara A., 2005, *ApJ*, 626, 627
- O'Shea B. W., Norman M. L., 2007, *ApJ*, 654, 66
- Palla F., Salpeter E. E., Stahler S. W., 1983, *ApJ*, 271, 632
- Peebles P. J. E., Dicke R. H., 1968, *ApJ*, 154, 891
- Prieto J., Jimenez R., Martí J., 2012, *MNRAS*, 419, 3092
- Prieto J., Jimenez R., Verde L., 2014, *MNRAS*, 437, 2320
- Ripamonti E., 2007, *MNRAS*, 376, 709
- Ripamonti E., Abel T., 2004, *MNRAS*, 348, 1019
- Saslaw W. C., Zipoy D., 1967, *Nature*, 216, 976
- Schleicher D. R. G., Banerjee R., Klessen R. S., 2008, *Phys. Rev. D*, 78, 083005
- Schleicher D. R. G., Latif M., Schober J., Schmidt W., Bovino S., Federrath C., Niemeyer J., Banerjee R., Klessen R. S., 2013, *Astronomische Nachrichten*, 334, 531
- Schleicher D. R. G., Schober J., Federrath C., Bovino S., Schmidt W., 2013, *New Journal of Physics*, 15, 023017
- Schneider R., Omukai K., Inoue A. K., Ferrara A., 2006, *MNRAS*, 369, 1437
- Schober J., Schleicher D., Federrath C., Glover S., Klessen R. S., Banerjee R., 2012, *ApJ*, 754, 99
- Shchekinov Y. A., Vasiliev E. O., 2006, *MNRAS*, 368, 454
- Smith R. J., Glover S. C. O., Clark P. C., Greif T., Klessen R. S., 2011, *MNRAS*, 414, 3633
- Stacy A., Bromm V., 2013, *arxiv:1307.1798*
- Stacy A., Greif T. H., Bromm V., 2012, *MNRAS*, 422, 290
- Stancil P. C., Lepp S., Dalgarno A., 1998, *ApJ*, 509, 1
- Tan J. C., McKee C. F., 2008, in O'Shea B. W., Heger A., eds, *First Stars III* Vol. 990 of American Institute of Physics Conference Series, *Star Formation at Zero and Very Low Metallicities*. pp 47–62
- The Enzo Collaboration Bryan G. L., et al. 2013, *arxiv:1307.2265*
- Truelove J. K., Klein R. I., McKee C. F., Holliman II J. H., Howell L. H., Greenough J. A., 1997, *ApJL*, 489, L179
- Turk M. J., Abel T., O'Shea B., 2009, *Science*, 325, 601
- Turk M. J., Smith B. D., Oishi J. S., Skory S., Skillman S. W., Abel T., Norman M. L., 2011, *ApJS*, 192, 9
- Volonteri M., 2012, *Science*, 337, 544
- Yoshida N., Oh S. P., Kitayama T., Hernquist L., 2007, *ApJ*, 663, 687
- Yoshida N., Omukai K., Hernquist L., Abel T., 2006, *ApJ*, 652, 6

This paper has been typeset from a \LaTeX file prepared by the author.